Phototoxicity in Human Retinal Pigment Epithelial Cells Promoted by Hypericin, a Component of St. John's Wort[†]

Albert R. Wielgus[1], Colin F. Chignell[1], David S. Miller[1], Ben Van Houten[2], Joel Meyer[2], Dan-Ning Hu[3] and Joan E. Roberts*[4]

[1]Laboratory of Pharmacology and Chemistry, National Institute of Environmental Health Sciences, Research Triangle Park, NC
[2]Laboratory of Molecular Genetics, National Institute of Environmental Health Sciences, Research Triangle Park, NC
[3]New York Eye and Ear Hospital, New York, NY
[4]Department of Natural Sciences, Fordham University, New York, NY

ABSTRACT

St. John's wort (SJW), an over-the-counter antidepressant, contains hypericin, which absorbs light in the UV and visible ranges. *In vivo* studies have determined that hypericin is phototoxic to skin and our previous *in vitro* studies with lens tissues have determined that it is potentially phototoxic to the human lens. To determine if hypericin might also be phototoxic to the human retina, we exposed human retinal pigment epithelial (hRPE) cells to 10^{-7} to 10^{-5} M hypericin. Fluorescence emission detected from the cells (λ_{ex} = 488 nm; λ_{em} = 505 nm) confirmed hypericin uptake by human RPE. Neither hypericin exposure alone nor visible light exposure alone reduced cell viability. However when irradiated with 0.7 J cm^{-2} of visible light (λ > 400 nm) there was loss of cell viability as measured by MTS and lactate dehydrogenase assays. The presence of hypericin in irradiated hRPE cells significantly changed the redox equilibrium of glutathione and a decrease in the activity of glutathione reductase. Increased lipid peroxidation as measured by the thiobarbituric acid reactive substances assay correlated to hypericin concentration in hRPE cells and visible light radiation. Thus, ingested SJW is potentially phototoxic to the retina and could contribute to retinal or early macular degeneration.

INTRODUCTION

Hypericin is a biologically active component of St. John's wort (SJW), an over-the-counter dietary supplement that has antidepressant properties (1,2). The *Hypericum perforatum* extract has also been associated with side effects and interactions with other drugs (3). The usual oral dose of SJW (1000 mg) produces a mean level of serum hypericin of 43 ng mL^{-1}, which is equivalent to a concentration of approximately 0.1 µM (4). When ingested or given by intra-vitreal injection for the photodynamic treatment of retinal neovascularization, hypericin accumulates in the retina at a concentration of 1–100 µM (5). Hypericin is known to be a very efficient photosensitizer when irradiated with either UV or visible light (6); both SJW and hypericin induce photosensitized erythema in the skin (7,8). The other potential target for phototoxic damage induced by hypericin is the eye (9).

Visible light (above 400 nm) is transmitted through the human lens to the retina (10). If this transmitted light interacts with an accumulated photosensitizer, it can damage both the human lens and the retina (9). Hypericin is capable of crossing the blood–retinal barrier (5), and has been shown to induce apoptosis in retinal pigment epithelial (RPE) (11) and human lens epithelial cells (12). We have previously determined that hypericin is taken up by the intact lens (13) and RPE cells (14), binds to (15) and damages lens proteins (16), and distorts the transmission of light through the lens (17). We report here a mechanism for the oxidative damage induced in human retinal pigment epithelial (hRPE) cells by hypericin in the presence of visible light.

MATERIALS AND METHODS

Reagents. 1-Chloro-2,4-dinitrobenzene, potassium chromate, potassium iodide and 2-vinylpyridine were purchased from Aldrich (Milwaukee, WI); glutathione reductase (GR) from baker's yeast from Fluka (Milwaukee, WI); gentamicin and trypsin from GIBCO (Grand Island, NY); sodium hydroxide and water from J.T. Baker (Phillipsburg, NJ); hydrochloric acid (~37%), anhydrous sodium carbonate, and trichloroacetic acid from Mallinckrodt (Paris, KY); and bovine albumin (fraction V), butylated hydroxytoluene, sterile dimethyl sulfoxide, 5,5′-dithiobis-(2-nitrobenzoic acid), EDTA, glutathione in both the reduced and oxidized forms, hypericin, NADPH, sodium nitrite, 5-sulfosalicylic acid (SSA), 2-thiobarbituric acid, triethanolamine, and Triton X-100 from Sigma (St. Louis, MO). All reagents used for experiments were at least analytical grade.

Cell cultures. The hRPE cells used in the present study were isolated from a donor eye (a 62-year-old male, cause of death: trauma) using the method of Hu *et al.* (18). The cells consisted of one cell line of a pure culture of cells in active growth status. The hRPE cells were distinguished from neighbor cells by immunocytochemical methods: hRPE cells displayed S-100 and cytokeratin, whereas uveal melanocytes displayed S-100 antigen but not cytokeratin, and fibroblasts displayed neither of these proteins (19).

The hRPE were cultured in Falcon flasks (75 cm^2) with Ham's F12 K and DMEM∕F-12 (2:1, vol∕vol) nutrient mixture supplemented with 10% fetal bovine serum (FBS), 2 mM L-glutamine and 50 µg mL^{-1} gentamicin. The confluent cells were detached by

0.125% trypsin solution, diluted by a factor of 3.6–13.2, and plated for subculture. The cells were cultured in 35 mm glass bottom microwell dishes (MatTek Culturware, Ashland, MA) for confocal microscopy, 96-well plates (Corning Incorporated, Corning, NY) for experiments where mitochondrial activity and lactate dehydrogenase (LDH) leakage were measured, and in 10 cm petri dishes (Becton Dickinson Labware, Franklin Lakes, NJ) before mitochondrial and nuclear DNA assays, determination of glutathione and thiobarbituric acid reactive substances (TBARS) concentrations, and measurement of glutathione S-transferase (GST) and GR activity. Cells were in the 13th– 22th passage.

Cell incubation with hypericin. Hypericin was dissolved in dimethyl sulfoxide (DMSO) and diluted with medium to the required concentrations immediately before addition to the cell culture. DMSO concentration was 0.1% in all cell culture plates including control samples. Cells were incubated in the dark at 37°C in a 5% CO_2/95% air atmosphere in medium without added chromophore (control cells) or containing 0.1–10 μM hypericin for 1–1½ h prior to light exposure. Cells were resuspended in phosphate-buffered saline (PBS) (pH 7.4, Ca^{2+} and Mg^{2+} free) or with PBS containing 10 mM glucose (PBS/Gluc).

Light exposure. The hRPE cells were exposed to light directly in the covered plates in which they were grown. The light source was two cool white visible light bulbs (Philips F40AX50, 40 W, 5000 K; Advantage X, Sommerset, NJ), with the light passed through a liquid filter (aqueous solution of $NaNO_2$ [50 g L^{-1}], K_2CrO_4 [0.2 g L^{-1}] and Na_2CO_3 [1 g L^{-1}]) transmitting light of wavelengths longer than 400 nm. The volume of the filter liquid in a 600 mL Falcon flask was carefully measured to get a vertical path length of exactly 1 cm in the horizontal position of the flask. Cells were irradiated for 1, 3, 5, and 10 min at a fluence rate of 10.6–12 W m^{-2}, which was monitored with an YSI-Kettering radiometer (model 65A; YSI, Yellow Springs, OH), equipped with a visible light photodiode. The maximal visible light dose was 0.72 J cm^{-2}, which is lower than the daily dose that reaches the human retina (20). Visible light dosages had no effect on the viability of the retinal cells. Control samples were kept in the dark under the same conditions.

Confocal microscopy. Human RPE cells were grown on glass cover slips that formed the floor of a Teflon microscope chamber. The cells were incubated in medium containing 0.5 or 1 μM hypericin for 1 h and were suspended in PBS/Gluc. Accumulation of hypericin in the RPE cells and the effect of light ($I = 12$ W m^{-2}) on the cells preincubated with the chromophore were observed using a Zeiss inverted confocal laser scanning microscope (Model 510 with multi-photon capabilities). To acquire images, the chamber containing the hRPE cells was mounted on the stage of the microscope and viewed through a 40× water immersion objective (NA 1.2). Excitation was provided by the 488 nm line of an Ar ion laser. A 505 nm long-pass emission filter was used. Low laser intensity was used to avoid photobleaching. With the photomultiplier gain set to give an average cellular fluorescence intensity of 50 (full scale, 255), hRPE autofluorescence due to endogenous lipofuscin was barely detectable.

Mitochondrial activity and cell membrane damage tests. After incubation of the cells with hypericin (0.1–10 μM) for 1½ h in medium, they were overlaid by PBS/Gluc and exposed to light. The buffer was then replaced with the medium and the cells were incubated in the dark at 37°C in a 5% CO_2/95% air atmosphere for 0.5–16 h, after which the MTS (3-(4,5-dimethylthiazol-2-yl)-5-(3-carboxymeth-oxyphenyl)-2-(4-sulfophenyl)-2H-tetrazolium, inner salt) and LDH assays were carried out. Mitochondrial activity was determined using MTS (Cell Titer 96® Aqueous Non-Radioactive Cell Proliferation Assay; Promega Corp., Madison, WI). Membrane damage was determined by LDH leakage, which was measured using CytoTox 96® Non-Radioactive Cytotoxicity Assay (Promega Corp.).

Mitochondrial and nuclear DNA assays. Directly after visible light exposure, irradiated cells and their dark controls were scraped out of plates with a cell lifter, suspended in PBS, and transferred to 15 mL plastic vials. Samples were centrifuged at 200 *g* for 5 min at 4°C. Supernatants were removed and cell precipitates were stored at −70°C until the assay.

Frozen cell pellets were later thawed and immediately transferred to 2 mL lysis buffer (Genomic-tips kit; Qiagen) supplemented with 4 μL RNase A (100 mg mL^{-1}; Qiagen) and 100 μL proteinase K (>600 mAU mL^{-1}; Qiagen). Samples were vortexed for 5 s and

incubated at 50°C for 2 h. Samples were then vortexed again for 10 s and loaded immediately onto pre-equilibrated Genomic-tip 20/G (Qiagen) columns. Subsequent purification of genomic DNA was carried out according to the Genomic-tips (Qiagen) protocol. The integrity of the extracted DNA was assessed by 1% agarose gel electrophoresis (30 V, 16 h).

Genomic DNA was quantitated using PicoGreen dye (Molecular Probes) as described by Santos *et al.* (21), and 15 ng of each sample was used as a template for PCR. PCR amplifications were performed as described by Santos *et al.* (21). In this assay, damage is detected as a decrease in amplification of the large genomic regions: lesions in a damaged template that significantly inhibit the progression of the polymerase will result in less PCR product, when the PCR is performed quantitatively. A small mitochondrial target is also amplified to correct for any variation in mitochondrial genome copy number. Because the target is very small, the possible presence of lesions will not have a significant effect on amplification. Damage to nuclear DNA was measured using primers 48510 and 62007 to amplify a noncoding region 5′ of the β-globin gene (13.75 kb), and damage to the mitochondrial genome was measured using primers 14841 and 5999 (large target; 8.9 kb) and 14841 and 14620 (small target; 221 bp). PCR mixtures and cycling conditions were essentially as described in Santos *et al.* (21); cycles of amplification were: β-globin, 26 cycles; large mitochondrial target, 18 cycles; small mitochondrial target, 19 cycles. PCR products were quantified with PicoGreen dye and a fluorescence plate reader, and lesion frequency was calculated by application of the Poisson distribution (22).

Preparation of cell samples for glutathione and TBARS assays. After about 1½ h dark incubation, the medium containing hypericin was removed. The cells in each plate were flushed twice with PBS and suspended in 5 mL of the buffer. Directly after light exposure, an aliquot of 325 μL of PBS supernatant was taken from each dish and transferred to separate tubes that each contained 325 μL of a 5% solution of SSA. The tube contents were mixed vigorously and placed on ice for protein precipitation. After 5 min incubation the samples were centrifuged at 10 000 *g* for 5 min at 4°C. Two 250 μL volumes of each supernatant were transferred to separate tubes for an assay of extracellular total glutathione (GSx) and its oxidized form (GSSG), respectively, and placed on dry ice. The remaining volume of PBS was removed and 0.5 mL HCl (10 mM) was added to each plate. The cells were scraped out of each plate, transferred to separate tubes and each was diluted with the HCl solution to 1 mL. A 600 μL portion of each cell suspension was transferred to empty tubes for the TBARS assay (23) and placed on dry ice. The remaining cell suspensions were sonicated (Ultrasonic Homogenizer 4710 Series; Cole-Parmer Instruments Co., Chicago, IL) for 10 s and centrifuged at 10 000 *g* for 5 min at 4°C. Fifty microliters of each supernatant was transferred to separate empty tubes for a protein assay and frozen. To prepare samples for intracellular glutathione determination, 325 μL of each cell supernatant was transferred to separate tubes that each contained 325 μL of 5% SSA. The samples were treated in a manner similar to that of the sample assigned for external glutathione determination. All samples were stored frozen at −70°C until further use.

Determination of extracellular and intracellular glutathione. Both extracellular and intracellular concentrations of GSx and GSSG were determined using the assay previously described by He *et al.* (24). The samples assigned for glutathione determination were thawed. A 200 μL aliquot of each previously prepared cell supernatant was placed in each of two empty tubes. Similarly, a 200 μL aliquot of each cell sample was transferred to separate empty tubes. Another 100 μL of each cell sample was added to 100 μL of a mixture of 5 mM HCl and 2.5% SSA. All samples were placed on ice. In the meantime standard solutions of the reduced form of glutathione (GSH) and GSSG were prepared. Then, 11 μL of 4 M triethanolamine solution was added to each tube to neutralize pH of the samples and mixed vigorously. To conjugate GSH, 4 μL of 2-vinylpyridine was added to each sample that was used for GSSG determination, mixed vigorously, and incubated at room temperature for 1 h. A 96-well plate was prepared by pipetting 50 μL of standard or sample per well. Immediately, 100 μL of freshly prepared assay cocktail (12.45 mL of 0.1 M phosphate buffer [pH 7.5] containing 10 mM EDTA, 0.4 mL of 10 mM NADPH, 0.5 mL of 6 mM 5,5′-dithiobis-[2-nitrobenzoic acid]

[DTNB], and 20 U of GR) were added to each well. The plate was stored in the dark for 15 min and absorbance at 405 nm was measured in a GENios plate reader (Tecan US SPECTRAFluor Plus, Research Triangle Park, NC). The concentration of GSH was calculated as GSH = GSx – 2·GSSG. The cellular redox state of intracellular glutathione was expressed as the ratio GSH/GSSG.

TBARS assay. The modified TBARS assay was used for lipid peroxidation monitoring (25). Samples assigned for the TBARS assay were thawed. Twenty microliters of 4.4 m*M* butylated hydroxytoluene followed by 10.2 μL of 10 *M* NaOH were added to each cell suspension. The samples were shaken at 60°C for 30 min. After cooling down, 170 μL of a mixture of 38% trichloroacetic acid and 2% KI were added to each sample, which was then mixed and placed on ice for 10 min. The samples were then centrifuged at 7000 *g* for 10 min at 4°C. A 350 μL aliquot of each supernatant was transferred to a new tube containing the same volume of 0.66% 2-thiobarbituric acid. The samples were mixed and incubated at 95°C for 30 min, then allowed to cool to room temperature. Absorbance was then registered at 534 nm (ε_{MDA} = 157 000 M^{-1} cm^{-1}) in a Hewlett Packard diode array 8453 spectrophotometer (Hewlett Packard GmbH, Waldbronn, Germany) using water as a reference.

Preparation of cell samples for determination of glutathione enzyme activity. After 1½ h of dark incubation with 10 μ*M* hypericin, medium was removed from the plates. The cells in each plate were washed twice with PBS and 8 mL of the buffer was added. Cells were then exposed to light or kept in the dark. For immediate analysis (t = 0) the supernatant was poured off; cells were scraped out directly after light exposure and suspended in 1 mL of ice-cold 0.1 *M* phosphate buffer (pH 7.0) containing 2 m*M* EDTA. To determine changes in enzyme activity over time, the PBS buffer during irradiation was replaced with 4 mL of medium and cells were incubated in the dark at 37°C in a 5% CO$_2$/95% air atmosphere for 0.5–4 h. Then after the incubation medium was removed, cells were washed twice with PBS, scraped out and suspended in the buffer as described above. Each cell suspension was homogenized using an Ultrasonic Homogenizer (Cole-Parmer, 4710 series) three times for 10 s each. Then all cell samples were centrifuged at 10 000 *g* for 15 min at 4°C. The cell supernatants were transferred to empty tubes and frozen until assay.

Glutathione S-transferase activity determination. The assay was performed in a 96-well plate. First 150 μL of 0.1 *M* phosphate buffer (pH 6.5) containing 0.1% Triton-X was transferred to each well. Then 20 μL of aqueous solution of 10 m*M* GSH and the same volume of a cell sample were added. The reaction was initiated by injection of 10 μL of 10 m*M* 1-chloro-2,4-dinitrobenzene (CDNB) in ethanol to each well. Absorbance change with time was recorded in the GENios plate reader at 340 nm. GST activity expressed as the rate constant of formation of GSH and CDNB product was calculated using ε_{340} = 9600 M^{-1} cm^{-1} and normalized to protein content.

Glutathione reductase activity determination. This assay was also performed in a 96-well plate. Ninety microliters of 75 m*M* phosphate buffer (pH 7.4) containing 1 m*M* EDTA (buffer-EDTA) was transferred to each well in the plate. Then 20 μL of 10 m*M* GSSG in buffer-EDTA was added, followed by 20 μL of a cell sample, and 50 μL of 10 m*M* DTNB in buffer-EDTA. The reaction was initiated by addition of 20 μL of 1 m*M* NADPH in buffer-EDTA to each well. The change in absorbance with time was recorded in the GENios plate reader at 415 nm. GR activity expressed as the rate constant of GSH and DTNB adduct formation was calculated using ϵ_{415} = 13 900 M^{-1} cm^{-1} and normalized to protein content.

Protein determination. Protein concentration was determined using bicinchoninic acid, Protein Assay Kit (Pierce, Rockford, IL). The assays were carried out in 96-well plates. Absorbance of the samples was measured at 560 nm in the GENios plate reader. Bovine albumin was used as a standard.

Statistical analysis. Data are presented as average ± SD of three to six experiments.

RESULTS

Confocal microscopy (ex 488 nm/em 505 nm) confirmed the uptake of hypericin in hRPE cells and its accumulation within both surface and interior membranes. Hypericin was detected
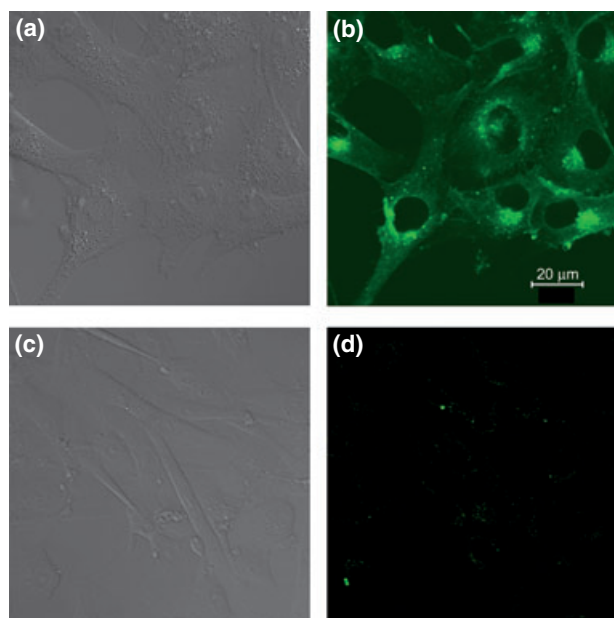

Figure 1. Hypericin is taken up by human retinal pigment epithelial (hRPE) cells and localizes predominantly in the Golgi apparatus. Confocal images of hRPE cells that were preincubated for 1 h in medium containing 1 μM hypericin and 0.1% DMSO (a, b) or 0.1% DMSO (c, d), then washed and overlaid with in PBS/Gluc. Images (a) and (c) show cells observed by transmitted light and (b) and (d) by fluorescence emission at λ_{em} = 505 nm (λ_{ex} = 488 nm) from the cells.

mainly in the Golgi apparatus and to some extent in cytoplasmic vesicles and the nuclear membrane. There was no evidence of hypericin uptake into the nucleus of the hRPE cells (Fig. 1).

In control cells not incubated with hypericin, exposure of up to 10 min of visible light had no effect on cell density or morphology. A 1-h dark incubation of hRPE cells in the presence of 1 μM hypericin also had no effect on cell density or morphology (Fig. 1). The cells remained attached to the plate and retained their characteristic appearance. There was no detectable damage to the hRPE cells after a 1-h incubation with 0.5 μM hypericin (Fig. 2a,b) followed by 1 min exposure to visible light (Fig. 2c,d). However, a 3-min exposure caused some morphological changes (Fig. 2e,f) in the hRPE cells and after 10 min of illumination most cells were round and some were partially fragmented (Fig. 2g,h). Ten-minute irradiation of the cells had no effect on fluorescence intensity of hypericin and the chromophore binding to intracellular structures of hRPE cells (Fig. 2b,d,f,h).

When hRPE cells were treated with 0.1–10 μM hypericin and irradiated with visible light for 10 min, there was a dose-dependent increase in the production of TBARS (Fig. 3), showing that lipid peroxidation had taken place.

Exposure to 1–10 μM hypericin and irradiation with visible light for 1–10 min caused a drug and light dose-dependent LDH leakage from the hRPE cells (Fig. 4).

When the hRPE cells were incubated at the highest dosages of hypericin (10 μM) and irradiated for 10 min, LDH leakage from the cells was observed after just 30 min (Fig. 5) and continued to increase during the 4 h it was measured. Such increasing leakage indicates severe cell membrane damage.
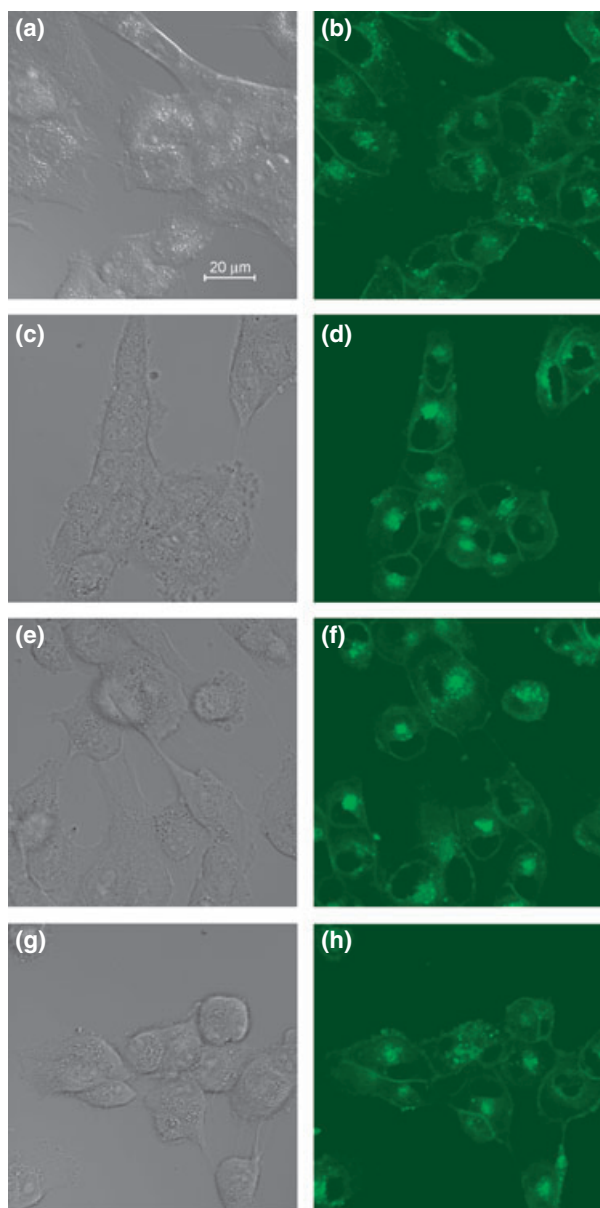
Figure 2. Visible light damages hypericin-exposed hRPE cells. After incubation in 0.5 μM hypericin, the cells were washed and overlaid with PBS/Gluc, and exposed to visible light ($\lambda > 400$ nm) for: (a, b) 0 min (dark control), (c, d) 1 min, (e, f) 3 min and (g, h) 10 min at a fluence rate of 12 W m^{-2}. Images (a), (c), (e) and (g) were recorded in transmitted light and images (b), (d), (f) and (h) show fluorescence emission at $\lambda_{em} = 505$ nm ($\lambda_{ex} = 488$ nm) from the cells.
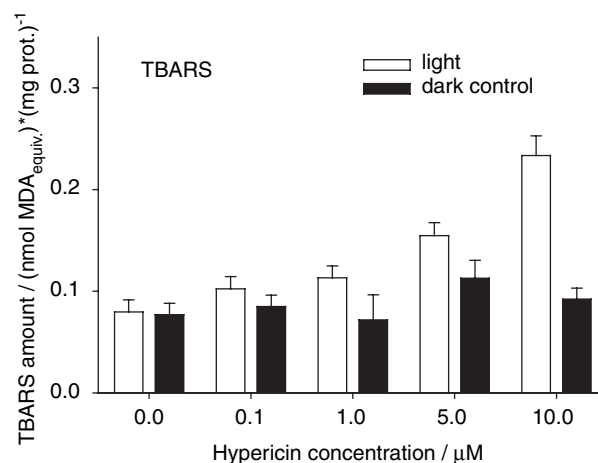

Figure 3. Visible light induces production of thiobarbituric acid reactive substances (TBARS) in hypericin-exposed hRPE cells. The cells were incubated in medium containing hypericin, washed twice and overlaid with PBS, exposed to light ($\lambda > 400$ nm, $I = 10.8$ W m^{-2}) for 10 min, scraped off directly after irradiation and frozen until the assay. The TBARS concentration was expressed as malondialdehyde equivalents and normalized to protein amount in the cells. Results are the average $\pm$ SD of three experiments.
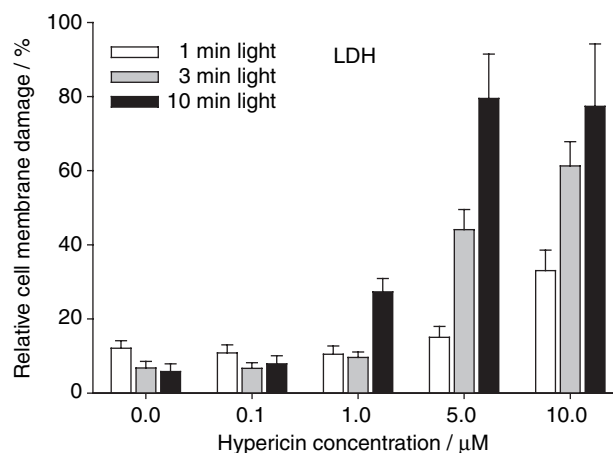

Figure 4. Visible light enhances cell membrane damage of hRPE cells containing hypericin as detected by lactate dehydrogenase (LDH) assay. The cells were incubated in the dark in medium containing 0.1–10 μM hypericin. Then they were washed twice and overlaid with PBS/Gluc, exposed to light ($\lambda > 400$ nm) at a fluence rate of 11.9 W m^{-2}, and the buffer was replaced with medium. The cells were incubated in the dark at 37°C in a 5% CO$_2$/95% air atmosphere for 16 h before the LDH assay. Percentage cell membrane damage was normalized to the cells treated in the same way and lysed directly before the assay. Results are the average $\pm$ SD of six experiments.

Cells incubated with hypericin (0.1–10 μM) and irradiated for 10 min with visible light exhibited significantly decreased intracellular total glutathione (GSx), as determined immediately after irradiation (Fig. 6a). Increasing concentrations of hypericin in the light-exposed cells led to a decrease in intracellular reduced glutathione (52.7 – 25.9 nmol mg^{-1} protein) (Fig. 6b) with a concomitant increase in its oxidized form (1.3 – 3.1 nmol mg^{-1} protein) (Fig. 6c) and decreased redox status (Fig. 6d). When cells were incubated with hypericin (0.1–10 μM) in the dark, there was no change in GSx levels (Fig. 6a).

Without hypericin, cells irradiated with visible light for 10 min underwent a slight increase in total glutathione levels (55.2 nmol mg^{-1} protein). The total glutathione levels in hRPE cells incubated in medium or suspended in PBS buffer in the dark were comparable (51.8 nmol mg^{-1} protein), with approximately 94% in the reduced form (data not shown).

Glutathione *S*-transferase activity was determined for hRPE cells incubated with 10 μM hypericin, irradiated for 10 min and measured at time points of 0–4 h. There was no significant change in the GST activity between the treated and
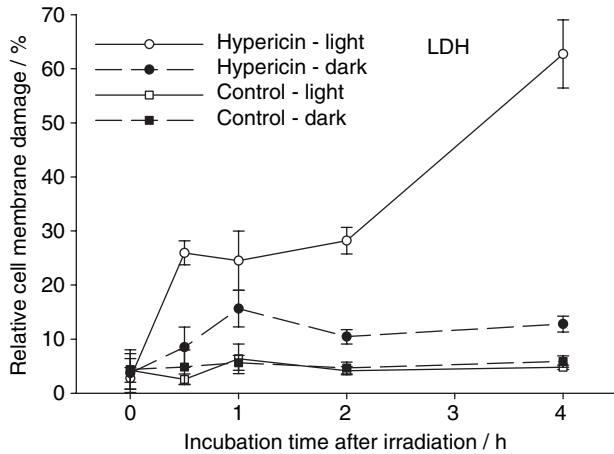
Figure 5. Visible light ($\lambda > 400$ nm) induces cell membrane damage in hypericin-exposed hRPE cells. The cells were incubated in the dark in medium containing 10 μM hypericin, washed twice and overlaid with PBS/Gluc, and irradiated for 10 min at a fluence rate of 11.6 W m^{-2}. After light exposure the cells were assayed immediately for lactate dehydrogenase (LDH) or reincubated in medium in the dark at 37°C in a 5% CO_2/95% air atmosphere for 0.5–4 h before the LDH assay. Damage to the cell membrane is expressed as a percentage determined from membrane damage of treated cells divided by the total damage induced by lysis. Results are the average ± SD of six experiments.

untreated hRPE cells (Fig. 7a). However, when GR activity was measured under the same conditions there was a distinct decrease in GR activity after 2 h post-light exposure incubation in medium (Fig. 7b).

Exposure to hypericin (1–10 μM) and then to visible light (1–10 min) caused a drug and light dose-dependent sharp decline in mitochondrial function, as assayed by MTS reduction after overnight incubation in medium (Fig. 8).

Mitochondrial activity also changed over time. When the hRPE cells were incubated with 10 μM hypericin, irradiated with visible light for 10 min, and re-incubated in medium for up to 4 h there was a time-dependent decrease in the MTS reduction rate (Fig. 9) that mimicked the LDH leakage from the cells (Fig. 5).

Exposure of hRPE cells to visible light and/or hypericin did not result in a detectable increase in either mitochondrial or nuclear DNA lesions compared to untreated cells. This was assessed with the QPCR assay, which uses quantitative PCR to examine the formation and repair of induced DNA damage in an 8.9-kb mitochondrial fragment and a 13.7-kb fragment flanking the β-globin gene (26) (data not shown).

DISCUSSION

We have demonstrated that exposure of hRPE cells to hypericin and visible light leads to an increase in polyunsaturated

Figure 6. Visible light depletes and oxidizes intracellular glutathione: (a) total (GSx), (b) reduced (GSH), and (c) oxidized (GSSG) form, and (d) the redox state in hRPE cells. The cells were incubated with hypericin, washed twice and overlaid with phosphate-buffered saline, exposed to light ($\lambda > 400$ nm, $I = 10.8$ W m^{-2}) for 10 min, scraped off immediately after irradiation, and prepared for the assay. Glutathione concentration was normalized to protein content. Results are the average ± SD of six experiments.
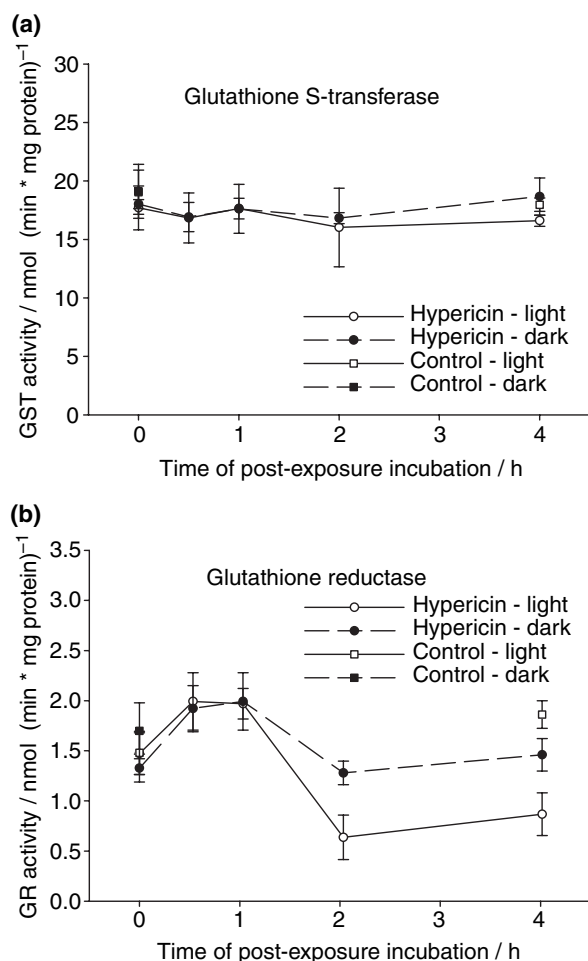
(a)

(b)
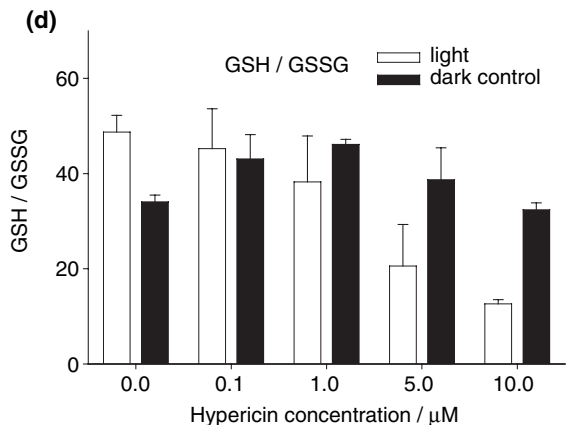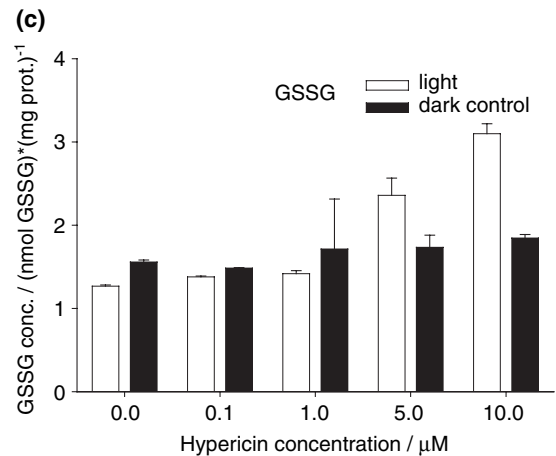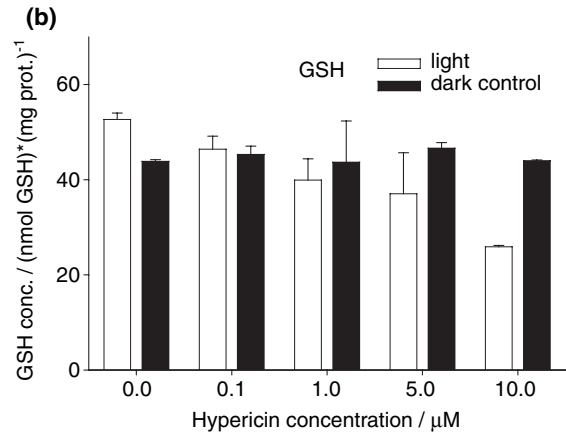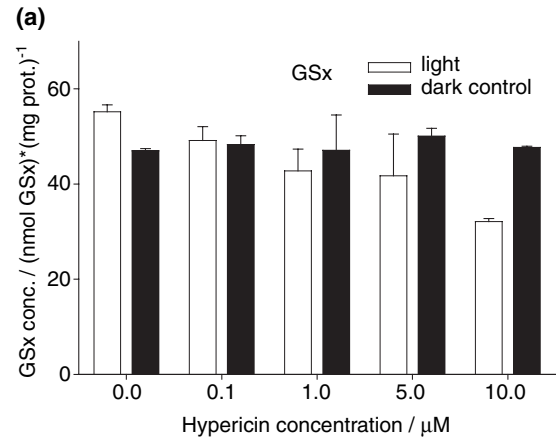
Figure 7. Glutathione *S*-transferase (GST) activity (a) is unaffected, and glutathione reductase (GR) activity (b) is reduced in hRPE cells exposed to 10 μM hypericin after 10 min visible light exposure. The cells were incubated in the dark in medium containing hypericin, washed twice and overlaid with phosphate-buffered saline, and exposed to light ($\lambda > 400$ nm) at a fluence rate of 11.6 W m^{-2}. The cells were then scraped off directly after irradiation or reincubated in medium in the dark at 37°C in a 5% CO$_2$/95% air atmosphere for 0.5–4 h, scraped off, and frozen until the assays. The enzyme activities were normalized to protein content in the cells. Results are the average ± SD of five experiments.

Figure 8. Mitochondrial activity is reduced in a dose-dependent fashion in hRPE cells exposed to hypericin and irradiated with visible light ($\lambda > 400$ nm). The cells were incubated in the dark in medium containing hypericin. They were then washed twice and overlaid with PBS/Gluc, irradiated at a fluence rate of 11.9 W m^{-2}, and the buffer was replaced with medium. The cells were incubated in the dark at 37°C in a 5% CO$_2$/95% air atmosphere for 16 h before the MTS assay. Percentage activities of mitochondria were normalized to control cells treated with hypericin but not irradiated. Results are the average ± SD of six experiments.

fatty acid oxidation and damage to the cell cytoplasmic membrane. Photoactivation of hypericin has also been found to induce either apoptosis or necrosis in HeLa cells (27) and lipid peroxidation in other cell lines (28–30). With age, increased lipid peroxidation exacerbates redox imbalance, leading to various chronic degenerative processes including vascular dysfunction (31). Lipid peroxidation is an important risk factor in the induction of retinal and choroidal neovascularization (wet macular degeneration) and diabetic retinopathy (32). The products of lipid peroxidation, particularly HNE (33) and AGE (34), are known to increase expression and secretion (35,36) of the angiogenesis growth factor VEGF by RPE cells.

The results of research performed on human glioma cells *in vitro* showed that photoactivation of hypericin leads to a depletion of intracellular glutathione (37). In these studies, we found that the photooxidation of hRPE by hypericin induced an intra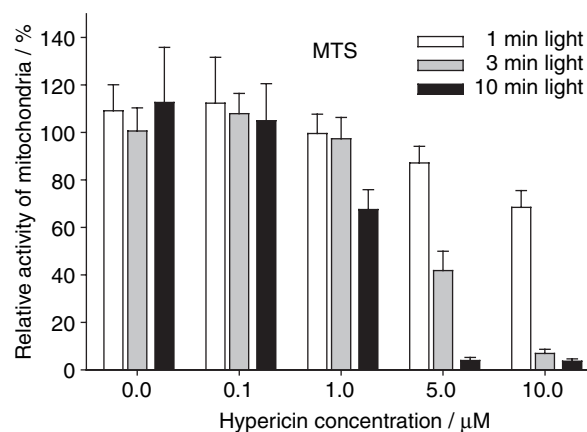cellular decrease in reduced glutathione (GSH) with a concomitant increase in its oxidized form (GSSG) and this was associated with lipid peroxidation (Fig. 10).

Any decrease in intracellular GSH induces oxidative stress in the hRPE cells (38). A decline of GSH in plasma or tissues has been associated with macular degeneration and diabetic retinopathy (39,40). GST is involved in detoxification of lipid hydroperoxides (41). *In vitro* studies of human nasopharyngeal cancer cells determined that photoactivation by hypericin down-regulates GST (42). However, we did not find a similar down-regulation of GST induced by photoactivation of hypericin with hRPE cells. GR reduces oxidized glutathione (GSSG) to its reduced form GSH. In this case, photoactivation of hypericin has been found to down-regulate GR in hRPE cells. This may be one explanation for the reduced level of total GSH and the increased level of oxidized glutathione.

Although DNA fragmentation was previously observed in RPE cells exposed to 2.5–5 μM hypericin, then irradiated for an hour, and incubated in medium containing 1% FBS (11), the pattern was typical of apoptosis. However, in our studies despite a reduction in mitochondrial activity, exposure of hRPE cells to visible light and/or hypericin did not result in a detectable increase in either mitochondrial or nuclear DNA lesions compared with untreated cells. Visible light exposure of RPE (11) and lens epithelial cells (12) pretreated with hypericin does induce apoptosis but probably through a lipid oxidation mechanism (43) rather than direct DNA damage.

In conclusion, we have determined that the photoactive component of SJW, hypericin, induces oxidative stress and lipid peroxidation in hRPE cells *in vitro*. There have been reports of the use of hypericin in conjunction with light therapy for treatment of depression (44). Hypericin is currently used as a diagnostic dye (45) and in photodynamic therapy for cancer (46) and ocular disorders (47). Because the level of hypericin reaching the RPE cells may be as high as 10–20 μM (47), these treatments may lead to oxidative
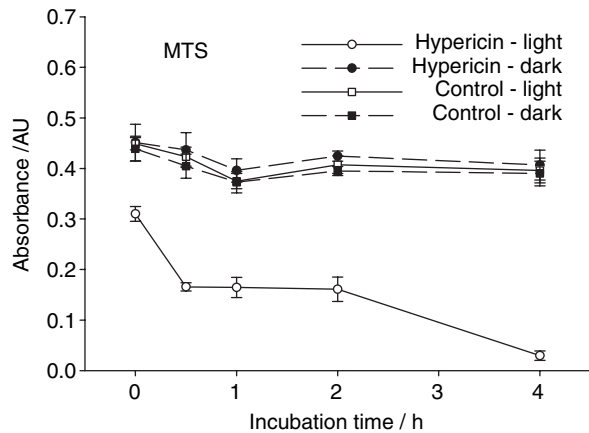
Figure 9. Visible light reduces mitochondrial activity in a time-dependent fashion in hypericin-exposed hRPE cells. The cells were incubated in the dark in medium containing 10 μM hypericin, washed twice and overlaid with PBS/Gluc, and exposed to light ($\lambda > 400$ nm) for 10 min at a fluence rate of 11.6 W m^{-2}. After irradiation the cells assayed immediately for MTS or reincubated in medium in the dark at 37°C in a 5% CO_2/95% air atmosphere for 0.5–4 h before the MTS assay. Results are the average ± SD of six experiments.
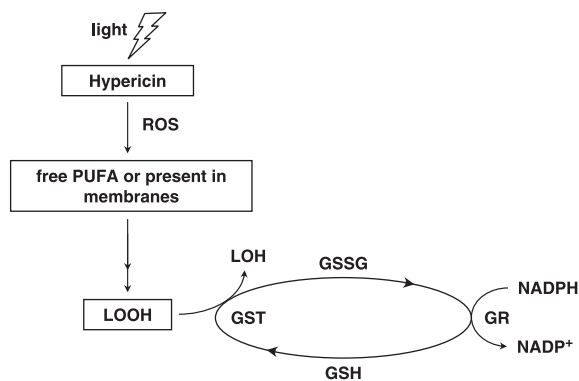

Figure 10. The scheme of lipid hydroperoxide (LOOH) detoxification by glutathione enzymes. Lipid hydroperoxides are normally reduced directly by glutathione S-transferase (GST) and indirectly by glutathione reductase (GR). However, photoactivation of hypericin in hRPE cells down-regulates GR, leading to a lower level of reduced form of glutathione (GSH) and increased level of both the oxidized form of glutathione (GSSG) and lipid hydroperoxides.

damage in the eye which could lead to transient or permanent blindness. Because the maximal light doses utilized in this study were lower than the daily dose that reaches the human retina, the current findings herein suggest that further studies need to be pursued intensively to more fully characterize the *in vivo* RPE cellular responses to hypericin and light exposure. Therefore at the moment, when this drug is taken, the eye must be protected from bright sunlight or intense artificial UV and visible light to avoid transient or permanent damage to the eye (9).

REFERENCES

1. Vitiello, B. (1999) *Hypericum perforatum* extracts as potential antidepressants. *J. Pharm. Pharmacol.* **51**, 513–517.
2. Whiskey, E., U. Werneke and D. Taylor (2001) A systematic review and meta-analysis of *Hypericum perforatum* in depression: A comprehensive clinical review. *Int. Clin. Psychopharmacol.* **16**, 239–252.
3. Final report on the safety assessment of *Hypericum perforatum* extract and *Hypericum perforatum* oil. (2001) *Int. J. Toxicol.* **20**, 31–39.
4. Schempp, C. M., B. Winghofer, M. Langheinrich, E. Schopf and J. C. Simon (1999) Hypericin levels in human serum and interstitial skin blister fluid after oral single-dose and steady-state administration of *Hypericum perforatum* extract (St. John's wort). *Skin Pharmacol. Appl. Skin Physiol.* **12**, 299–304.
5. Higuchi, A. H., H. Yamada, E. Yamada and M. Matsumura (2003) Inhibitory effect of hypericin on retinal and choroidal neovascularization. *Invest. Ophthalmol. Vis. Sci.* **44**, E-Abstract 554.
6. Ehrenberg, B., J. L. Anderson and C. S. Foote (1998) Kinetics and yield of singlet oxygen photosensitized by hypericin in organic and biological media. *Photochem. Photobiol.* **68**, 135–140.
7. Gulick, R. M., V. McAuliffe, J. Holden-Wiltse, C. Crumpacker, L. Liebes, D. S. Stein, P. Meehan, S. Hussey, J. Forcht and F. T. Valentine (1999) Phase I studies of hypericin, the active compound in St. John's wort, as an antiretroviral agent in HIV-infected adults. AIDS Clinical Trials Group Protocols 150 and 258. *Ann. Intern. Med.* **130**, 510–514.
8. Cotterill, J. A. (2001) Severe phototoxic reaction to laser treatment in a patient taking St John's wort. *J. Cosmet. Laser Ther.* **3**, 159–160.
9. Roberts, J. E. (2002) Screening for ocular phototoxicity. *Int. J. Toxicol.* **21**, 491–500.
10. Barker, F. M., G. C. Brainard and P. Dayhaw-Barker (1991) Transmission of the human lens as a function of age. *Invest. Ophthalmol. Vis. Sci.* **32S**, 1083.
11. Harris, M. S., T. Sakamoto, H. Kimura, S. He, C. Spee, R. Gopalakrishna, U. Gundimeda, J. S. Yoo, D. R. Hinton and S. J. Ryan (1996) Hypericin inhibits cell growth and induces apoptosis in retinal pigment epithelial cells: Possible involvement of protein kinase C. *Curr. Eye Res.* **15**, 255–262.
12. He, Y.-Y., C. F. Chignell, D. S. Miller, U. P. Andley and J. E. Roberts (2004) Phototoxicity in human lens epithelial cells promoted by St. John's wort. *Photochem. Photobiol.* **80**, 583–586.
13. Sgarbossa, A., N. Angelini, D. Gioffre, T. Youssef, F. Lenci and J. E. Roberts (2000) The uptake, location and fluorescence of hypericin in bovine intact lens. *Curr. Eye Res.* **21**, 597–601.
14. Taroni, P., G. Valentini, D. Comelli, C. D'Andrea, R. Cubeddu, D.-N. Hu and J. E. Roberts (2005) Time-resolved microspectrofluorimetry and fluorescence lifetime imaging of hypericin in human retinal pigment epithelial cells. *Photochem. Photobiol.* **81**, 524–528.
15. Sgarbossa, A., T. Youssef and F. Lenci (2003) Photosensitized structural modifications of the lens protein alpha-crystallin: Do all modifications impair chaperone-like activity? *Photochem. Photobiol.* **77**, 567–571.
16. Schey, K. L., S. Patat, C. F. Chignell, M. Datillo, R. H. Wang and J. E. Roberts (2000) Photooxidation of lens alpha-crystallin by hypericin (active ingredient in St. John's wort). *Photochem. Photobiol.* **72**, 200–203.
17. Wahlman, J., M. Hirst, J. E. Roberts, C. D. Prickett and J. R. Trevithick (2003) Focal length variability and protein leakage as tools for measuring photooxidative damage to the lens. *Photochem. Photobiol.* **78**, 88–92.
18. Hu, D.-N., H. E. Savage and J. E. Roberts (2002) Uveal melanocytes, ocular pigment epithelium, and Mueller cells in culture: In vitro toxicology. *Int. J. Toxicol.* **21**, 465–472.
19. Hu, D.-N., S. A. McCormick, R. Ritch and K. Pelton-Henrion (1993) Studies of human uveal melanocytes in vitro: Isolation, purification and cultivation of human uveal melanocytes. *Invest. Ophthalmol. Vis. Sci.* **34**, 2210–2219.
20. Sliney, D. H. (2002) How light reaches the eye and its components. *Int. J. Toxicol.* **21**, 501–509.

21. Santos, J. H., B. S. Mandavilli and B. Van Houten (2002) Measuring oxidative mtDNA damage and repair using quantitative PCR. *Methods Mol. Biol.* **197**, 159–176.
22. Ayala-Torres, S., Y. Chen, T. Svoboda, J. Rosenblatt and B. Van Houten (2000) Analysis of gene-specific DNA damage and repair using quantitative polymerase chain reaction. *Methods* **22**, 135–147.
23. Janero, D. R. (1990) Malondialdehyde and thiobarbituric acid-reactivity as diagnostic indices of lipid peroxidation and peroxidative tissue injury. *Free Radic. Biol. Med.* **9**, 515–540.
24. He, Y.-Y., J.-L. Huang, D. C. Ramirez and C. F. Chignell (2003) Role of reduced glutathione efflux in apoptosis of immortalized human keratinocytes induced by UVA. *J. Biol. Chem.* **278**, 8058–8064.
25. Hong, Y.-L., S.-L. Yeh, C.-Y. Chang and M.-L. Hu (2000) Total plasma malondialdehyde levels in 16 Taiwanese college students determined by various thiobarbituric acid tests and an improved high-performance liquid chromatography-based method. *Clin. Biochem.* **33**, 619–625.
26. Yakes, F. M. and B. Van Houten (1997) Mitochondrial DNA damage is more extensive and persists longer than nuclear DNA damage in human cells following oxidative stress. *Proc. Natl Acad. Sci. USA* **94**, 514–519.
27. Vantieghem, A., Z. Assefa, P. Vandenabeele, W. Declercq, S. Courtois, J. R. Vandenheede, W. Merlevede, P. de Witte and P. Agostinis (1998) Hypericin-induced photosensitization of HeLa cells leads to apoptosis or necrosis: Involvement of cytochrome c and procaspase-3 activation in the mechanism of apoptosis. *FEBS Lett.* **440**, 19–24.
28. Hadjur, C., M. J. Richard, M. O. Parat, P. Jardon and A. Favier (1996) Photodynamic effects of hypericin on lipid peroxidation and antioxidant status in melanoma cells. *Photochem. Photobiol.* **64**, 375–381.
29. Andreoni, A., A. Colasanti, P. Colasanti, M. Mastrocinque, P. Riccio and G. Roberti (1994) Laser photosensitization of cells by hypericin. *Photochem. Photobiol.* **59**, 529–533.
30. Du, H. Y., M. Olivo, B. K. Tan and B. H. Bay (2003) Hypericin-mediated photodynamic therapy induces lipid peroxidation and necrosis in nasopharyngeal cancer. *Int. J. Oncol.* **23**, 1401–1405.
31. Lee, J. Y., J. H. Je, D. H. Kim, S. W. Chung, Y. Zou, N. D. Kim, M. Ae Yoo, H. Suck Baik, B. P. Yu and H. Y. Chung (2004) Induction of endothelial apoptosis by 4-hydroxyhexenal. *Eur. J. Biochem.* **271**, 1339–1347.
32. Hardy, P., M. Beauchamp, F. Sennlaub, F. Gobeil Jr, L. Tremblay, B. Mwaikambo, P. Lachapelle and S. Chemtob (2005) New insights into the retinal circulation: Inflammatory lipid mediators in ischemic retinopathy. *Prostaglandins Leukot. Essent. Fatty Acids* **72**, 301–325.
33. Ayalasomayajula, S. P. and U. B. Kompella (2002) Induction of vascular endothelial growth factor by 4-hydroxynonenal and its prevention by glutathione precursors in retinal pigment epithelial cells. *Eur. J. Pharmacol.* **449**, 213–220.
34. Fu, M. X., J. R. Requena, A. J. Jenkins, T. J. Lyons, J. W. Baynes and S. R. Thorpe (1996) The advanced glycation end product, Nepsilon-(carboxymethyl)lysine, is a product of both lipid peroxidation and glycoxidation reactions. *J. Biol. Chem.* **271**, 9982–9986.
35. Lu, M., M. Kuroki, S. Amano, M. Tolentino, K. Keough, I. Kim, R. Bucala and A. P. Adamis (1998) Advanced glycation end products increase retinal vascular endothelial growth factor expression. *J. Clin. Invest.* **101**, 1219–1224.
36. Treins, C., S. Giorgetti-Peraldi, J. Murdaca and E. Van Obberghen (2001) Regulation of vascular endothelial growth factor expression by advanced glycation end products. *J. Biol. Chem.* **276**, 43836–43841.
37. Miccoli, L., A. Beurdeley-Thomas, G. De Pinieux, F. Sureau, S. Oudard, B. Dutrillaux and M. F. Poupon (1998) Light-induced photoactivation of hypericin affects the energy metabolism of human glioma cells by inhibiting hexokinase bound to mitochondria. *Cancer Res.* **58**, 5777–5786.
38. Jiang, S., S. E. Moriarty-Craige, M. Orr, J. Cai, P. Sternberg Jr and D. P. Jones (2005) Oxidant-induced apoptosis in human retinal pigment epithelial cells: Dependence on extracellular redox state. *Invest. Ophthalmol. Vis. Sci.* **46**, 1054–1061.
39. Coral, K., R. Raman, S. Rathi, M. Rajesh, K. N. Sulochana, N. Angayarkanni, P. G. Paul and S. Ramakrishnan (2006) Plasma homocysteine and total thiol content in patients with exudative age-related macular degeneration. *Eye* **20**, 203–207.
40. Samiec, P. S., C. Drews-Botsch, E. W. Flagg, J. C. Kurtz, P. Sternberg Jr, R. L. Reed and D. P. Jones (1998) Glutathione in human plasma: Decline in association with aging, age-related macular degeneration, and diabetes. *Free Radic. Biol. Med.* **24**, 699–704.
41. Ketterer, B. and D. J. Meyer (1989) Glutathione transferases: A possible role in the detoxication and repair of DNA and lipid hydroperoxides. *Mutat. Res.* **214**, 33–40.
42. Du, H. Y., M. Olivo, B. K. Tan and B. H. Bay (2004) Photoactivation of hypericin down-regulates glutathione S-transferase activity in nasopharyngeal cancer cells. *Cancer Lett.* **207**, 175–181.
43. Poli, G. and R. J. Schaur (2000) 4-Hydroxynonenal in the pathomechanisms of oxidative stress. *IUBMB Life* **50**, 315–321.
44. Wheatley, D. (1999) Hypericum in seasonal affective disorder (SAD). *Curr. Med. Res. Opin.* **15**, 33–37.
45. Zaak, D., A. Karl, R. Knuchel, H. Stepp, A. Hartmann, O. Reich, A. Bachmann, M. Siebels, G. Popken and C. Stief (2005) Diagnosis of urothelial carcinoma of the bladder using fluorescence endoscopy. *BJU Int.* **96**, 217–222.
46. Huygens, A., A. R. Kamuhabwa, A. Van Laethem, T. Roskams, B. Van Cleynenbreugel, H. Van Poppel, P. Agostinis and P. A. De Witte (2005) Enhancing the photodynamic effect of hypericin in tumour spheroids by fractionated light delivery in combination with hyperoxygenation. *Int. J. Oncol.* **26**, 1691–1697.
47. Weinberger, D., Y. Ron, M. Lusky, D. Gaaton, A. Orenstein, M. Blank, M. Mandel, T. Livnat, T. Barliya and G. Lavie (2005) Competitive quenching: A possible novel approach in protecting RPE cells from damage during PDT. *Curr. Eye Res.* **30**, 269–277.